Brain Network Evaluation by Functional-Guided Effective Connectivity Reinforcement Learning Method Indicates Therapeutic Effect for Tinnitus

Han Lv, Jinduo Liu, *Member, IEEE*, Qian Chen, Junzhong Ji, Jihao Zhai, Zuozhen Zhang, Zhaodi Wang, Shusheng Gong, and Zhenchang Wang

***Abstract*— Using functional connectivity (FC) or effective connectivity (EC) alone cannot effectively delineate brain networks based on functional magnetic resonance imaging (fMRI) data, limiting the understanding of the mechanism of tinnitus and its treatment. Investigating brain FC is a foundational step in exploring EC. This study proposed a functionally guided EC (FGEC) method based on reinforcement learning (FGECRL) to enhance the precision of identifying EC between distinct brain regions. An actor–critic framework with an encoder–decoder model was adopted as the actor network. The encoder utilizes a transformer model; the decoder employs a bidirectional long short-term memory network with attention. An FGEC network was constructed for the enrolled participants per fMRI scan, including 65 patients with tinnitus and 28 control participants healthy at the enrollment time. After 6 months of sound therapy for tinnitus and prospective follow-up, fMRI data were acquired again and retrospectively categorized into an effective group (EG) and an ineffective group (IG) according to the treatment effect. Compared with FC and EC, the FGECRL method demonstrated better accuracy in discriminating between different groups, highlighting the advantage of FGECRL in identifying brain network features. For the FGEC network of the EG and IG per state (before and after treatment) and healthy controls, effective therapy is characterized by a similar pattern of FGEC network between patients with tinnitus after treatment and healthy controls. Deactivated information output in the motor network, somatosensory network, and medioventral occipital cortex may biologically indicate effective treatment. The maintenance of decreased EC in the primary auditory cortex may represent a failure of sound therapy, further supporting the Bayesian inference theory for tinnitus perception. The FGEC network can provide direct evidence for the mechanism of sound therapy in patients with tinnitus with distinct outcomes.**

***Index Terms*— Tinnitus, sound therapy, fMRI, brain network, reinforcement learning.**

I. Introduction

TINNITUS occurs in up to 25% people worldwide [1]. Continuous bothersome noise can lead to a significantly greater likelihood of suicide because of anxiety, depression, or sleep disorders [2]. Tinnitus treatment is of great concern. According to the evidence-based guidelines for treating tinnitus [3], sound therapy is a recommended treatment that can be commonly used in clinics.

However, doctors always encounter unsatisfactory treatment effects from sound therapy in the clinic. It was reported that approximately 20% to 40% of patients respond poorly to months of treatment [4], [5]. Moreover, sound therapy is time consuming. In general, at least four weeks are needed before determine the effect of treatment. Thus, it is valuable if there is a way to character tinnitus patients with different treatment outcomes before sound therapy. Non-responders may be suggested to try another kind of treatment without delay. We can also try to analyze the mechanism of tinnitus with objective evidence.

Functional magnetic resonance imaging (fMRI) studies can provide objective evidence for the analysis of tinnitus. Previous fMRI studies indicated that tinnitus is characterized

Manuscript received 14 November 2023; revised 30 January 2024; accepted 29 February 2024. Date of publication 7 March 2024; date of current version 12 March 2024. The work of Han Lv was supported in part by the National Natural Science Foundation of China under Grant 62171297 and in part by Beijing Natural Science Foundation under Grant 7242267. The work of Jinduo Liu was supported by the National Natural Science Foundation of China under Grant 62106009. The work of Junzhong Ji was supported by the National Natural Science Foundation of China under Grant 62276010. The work of Zhenchang Wang was supported by the National Natural Science Foundation of China under Grant 61931013. *(Corresponding author: Jinduo Liu.)*

This work involved human subjects or animals in its research. Approval of all ethical and experimental procedures and protocols was granted by Beijing Friendship Hospital, Capital Medical University under Application No. 2018-P2-182-01.

Han Lv, Qian Chen, and Zhenchang Wang are with the Department of Radiology, Beijing Friendship Hospital, Capital Medical University, Beijing 100050, China (e-mail: chrislvhan@126.com).

Jinduo Liu, Junzhong Ji, Jihao Zhai, and Zuozhen Zhang are with Beijing Municipal Key Laboratory of Multimedia and Intelligent Software Technology, Faculty of Information Technology, Beijing University of Technology, Beijing 100124, China (e-mail: jinduo@bjut.edu.cn).

Zhaodi Wang and Shusheng Gong are with the Department of Otolaryngology Head and Neck Surgery, Beijing Friendship Hospital, Capital Medical University, Beijing 100050, China.

This article has supplementary downloadable material available at https://doi.org/10.1109/TNSRE.2024.3373335, provided by the authors.

Digital Object Identifier 10.1109/TNSRE.2024.3373335

by abnormal functional activity in the central nervous system [6]. Functional connectivity (FC) plays a vital role in understanding the interconnections between brain regions in patients with tinnitus [7], [8], [9]. Effective treatment may alter the topological features of the brain network [10], [11], and effective connectivity (EC) has become a cutting-edge research topic [12]. The elucidation of the brain's EC network prior to tinnitus treatment [13] advances our understanding of the tinnitus mechanism because of its better description of the brain's directed information flow. However, FC or EC alone may not fully characterize the features of brain networks.

Several novel brain EC learning methods based on deep learning techniques have been proposed, offering significant advantages over traditional machine learning methods in handling noisy and nonlinear data [14], [15]. Liu et al. proposed an algorithm that employs generative adversarial networks (GANs) to model brain EC networks (EC-GAN). The generator utilizes structural equation models to quantify the causal relationships among brain regions; the discriminator distinguishes between the joint distribution of real and generated fMRI time series [16], [17]. Li et al. introduced causal recurrent variational autoencoder (CR-VAE), a method that learns EC using an encoder and multihead decoders, embracing the general concept of Granger causality typically used in FC analysis [18]. These advancements demonstrate the potential of deep learning approaches in brain EC analysis.

We hypothesized that FGEC would be a better tool to identify the feature of functional connectivity than FC or EC alone, thus it would identify the neural activity feature of tinnitus with distinct outcomes. This study advocates implementing an assisted learning mechanism to enhance the precision of the brain's EC network, leveraging FC as a guide for estimating EC using a novel deep learning method.

This approach leverages the excellent optimization and noise-resistance capabilities of reinforcement learning, potentially uncovering different underlying brain network patterns in patients with tinnitus and healthy individuals. An EC network that integrates FC information can be expected to delineate the brain network more effectively than the performance of an FC or EC network alone. This study elucidates the mechanism of tinnitus from the perspective of directed information flow in brain networks.

II. Materials

This study was registered on ClinicalTrials.gov (ID. NCT03764826). Our research was approved by the ethics committees of Beijing Friendship Hospital, Capital Medical University (ID. 2018-P2-182-01). Written informed consent was obtained from all study subjects.

A. Participants

All participants were prospectively enrolled in the study. The inclusion criteria were (1) age between 18 and 70 years, (2) right-handed, and (3) no contraindications to MRI acquisition. Tinnitus patients needed to be willing to be treated and followed-up for 6 months. The exclusion criteria were (1) history of tinnitus treatment, (2) hyperacusis, head trauma, suspected Meniere's disease, or other neurological diseases, and (3) cerebral focal lesions. Ultimately, 65 patients with non-pulsatile tonal-like tinnitus and 28 healthy control (HC) participants were enrolled. None of the participants was excluded.

B. Sound Therapy and Treatment Effects Evaluation

All patients with tinnitus were examined for tinnitus frequency (Tf), minimum masking levels, tinnitus pitch matching, and loudness matching (L). The narrowband sound used for the treatment was set by an otologist (with more than 10 years of tinnitus treatment experience) from our institution. The loudness was set at 5 dB lower than the loudness matching. The bandwidth was set according to Tf and was 1/3 of an octave. Patients received sound therapy for 20 minutes per session, three sessions per day, for 24 weeks using headphones and SpeechEasy eMasker (Micro-DSP Technology Co., Ltd., China). The HCs did not receive any intervention.

For patients with tinnitus, the Tinnitus Handicap Inventory (THI) score was acquired before and after treatment the same day before MRI data acquisition. THI is a self-reported measure commonly used to evaluate tinnitus severity. Effective treatment was defined as a more than 17 point reduction in the THI score or a THI score reduced to less than 16 points [19]. Based on the treatment effect, patients were categorized into an effective treatment group (ET) or an ineffective treatment group (IT). Changes were calculated for the THI score and percentage improvement in the THI score (absolute change in the THI value divided by the value at baseline).

C. Medical Imaging Data Acquisition and Preprocessing

MRI data of the patients and HCs were acquired at the enrollment time. Patients were also scanned at the 24th week after treatment; the HCs were scanned after 24 weeks of follow-up. For all subjects, data were obtained using a 3.0T MRI system (Prisma; Siemens, Erlangen, Germany) with a 64-channel phase-array head coil. We acquired high spatial resolution T1-weighted images and blood oxygenation level–dependent resting-state fMRI (rs-fMRI). The fMRI scanning parameters were: 240 total number volumes; 33 slices; slice thickness/gap = 3.5 mm/1 mm; repetition time (TR)/echo time (TE) = 2000 ms/30 ms; matrix = 64 × 64; field of view = 224 × 224 mm^2.

Data preprocessing was performed using SPM 12 (http://www.fil.ion.ucl.ac.uk/spm) and the Graph–theoretical Network Analysis Toolkit (GRETNA, http://www.nitrc.org/projects/gretna/) [20] installed in MATLAB 2016a (MathWorks; Natick, MA, USA). The first ten volumes of rs-fMRI data were discarded. In brief, we performed slice timing, realignment, spatial normalization into the Montreal Neurological Institute template using T1-weighted imaging, resampling to 3 × 3 × 3 mm voxels, smoothing using a 6 mm full-width at half maximum Gaussian kernel, detrending temporal filtering (0.01– 0.1 Hz), and segmentation according to a brain atlas that included 246 sub-brain regions [21]. The time series of each region of interest (ROI) was extracted.

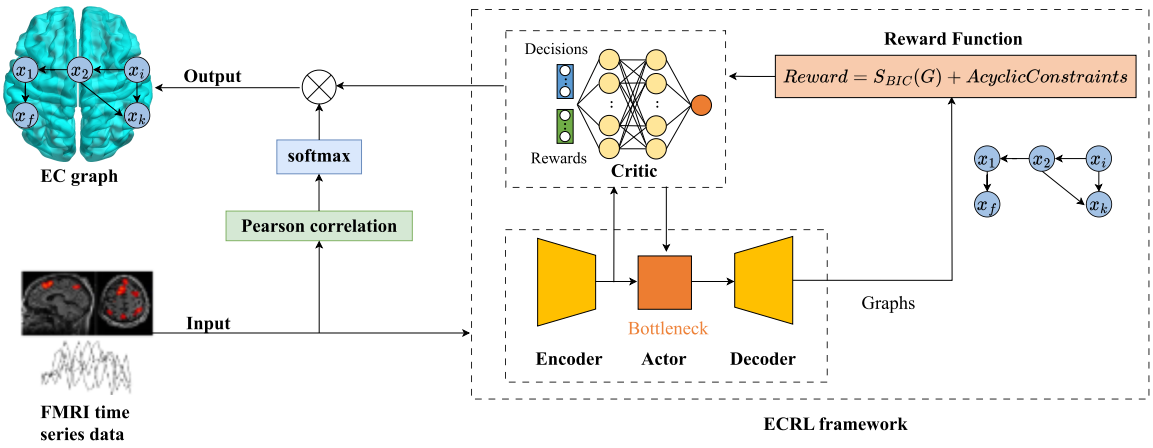

Fig. 1. The architecture of the proposed method FGECRL.

III. Methodology

Our innovative model (FGECRL) estimates effective brain connectivity through reinforcement learning (ECRL), incorporating FC guidance from fMRI time-series data. We provide a comprehensive overview of the FGECRL and a detailed exploration of its core components below.

A. The Architecture of FGECRL

The FGECRL approach integrates the actor–critic algorithm into learning effective brain connectivity while leveraging FC as guidance. By comparing the three pivotal components, namely, the *actor*, *critic*, and *reward*, the comprehensive structure of the FGECRL framework is visualized in Figure 1. The following sections provide a comprehensive breakdown of each of these three components.

B. Actor

The actor component within the FGECRL was formulated as an encoder–decoder model crafted to accept noise variables and authentic fMRI time-series data as inputs. Its purpose is to produce directed graphs manifested as graph adjacency matrices representing effective brain connectivity networks. Given its innate capability to extract contextual insights, this encoder–decoder model is particularly suitable for handling fMRI time-series data. The next section presents an intricate breakdown of the implemented Encoder and Decoder components.

1) Encoder: In FGECRL, we integrate a Transformer-based encoder. The schematic of this encoder's architecture is illustrated in Figure 2.

The initial step in the encoder process embeds the inputs through a linear layer. The derived embedded inputs proceed through numerous identical encoder blocks. Each encoder block comprises a multihead self-attention layer and a feedforward layer. Recent research has underscored the efficacy of multihead self-attention in extracting valuable insights from fMRI data, encompassing both temporal and spatial features. This mechanism diminishes the need for external information and enhances the capacity to capture intrinsic correlations within the dataset. In our setting, we use three feedforward

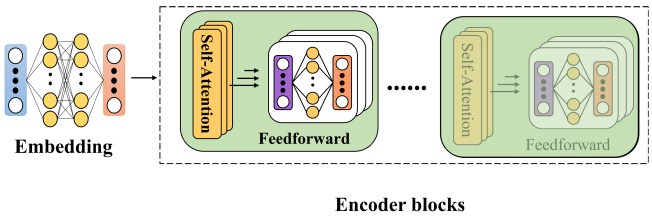

Fig. 2. Encoder architecture.

layers for input embedding. For each encoder block, We set the number of heads for multi-head attention to 16, and the number of hidden layer nodes is 256. We stack 6 encoder blocks together to effectively extract the spatio-temporal features of fMRI. For the fMRI data X, the operations within the encoder blocks for the fMRI data X can be described as follows:

$$\begin{aligned} Q_h &= W^Q X'^h + bias^Q, \\ K_h &= W^K X'^h + bias^K, \\ V_h &= W^V X'^h + bias^V, \end{aligned} \tag{1}$$

where X'^h represents the h-th input, achieved by partitioning the embedded input X' into H groups. The attention mechanism can be described as a function that takes both a value and a set of key-query pairs as input and produces an output by calculating a weighted sum of the values. Q, K and V describe the query, key, and value, Q, K is used to calculate the similarity of the input features and acquire the attention features with value V. W^Q, W^K and W^V denote the network parameters for the self-attention layer, respectively, $bias^Q$, $bias^K$, and $bias^V$ are the bias vector. The computation of multi-head self-attention follows this formulation:

$$SelfAtt_h = softmax\left(\frac{Q_h {K_h}^t}{\sqrt{D_{K_h}}}\right) V_h, \tag{2}$$

where D denotes the count of elements in the last dimension of K. We then derive multi-head attention by concatenating all H sets of self-attention, leading to the following expression:

$$MultiHead = Concat(SelfAtt_1, \ldots, SelfAtt_H). \tag{3}$$

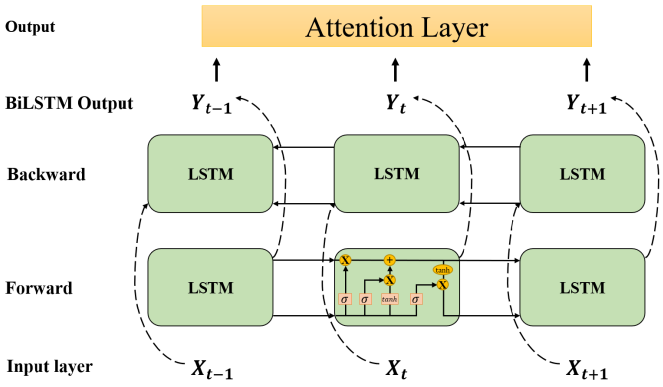

Fig. 3. Decoder architecture.

Subsequently, the outcome of the multi-head attention process is passed through a feedforward layer comprising two linear layers and a ReLU activation function.

$$Block = ReLU(MultiHeadW_1 + bias_1)W_2 + bias_2. \quad (4)$$

2) Decoder: The decoder utilizes the Bi-directional Long Short-Term Memory (BiLSTM) architecture, complemented by an attention layer. This selection is motivated by the BiLSTM's effectiveness in capturing global information and addressing gradient vanishing or exploding concerns during extended sequence training. The BiLSTM model encompasses numerous LSTM cells, and its comprehensive structure is visually depicted in Figure 3.

The BiLSTM model encompasses two distinct layers: the forward layer and the backward layer. Each layer is set to 16 hidden nodes. For the attention layer, the input dimension is twice the output dimension of the BiLSTM module, and the number of hidden layer nodes is set to 256. In detail, the forward layer, operating from time step 1 to T, refines the long-term memory and preserves the hidden state. When provided with the encoder output enc_t from the t-th time step, the hidden state can be characterized as follows:

$$\overrightarrow{H_t} = f(enc_t {W_1}^{(f)} + \overrightarrow{H_{t-1}} {W_2}^{(f)} + {bias}^{(f)}), \quad (5)$$

where ${W_1}^{(f)}$, ${W_2}^{(f)}$, and ${bias}^{(f)}$ correspond to the parameters of the forward layer, with the function f representing the LSTM model. The process of the backward layer mirrors that of the forward layer, albeit with the time step ranging from T down to 1:

$$\overleftarrow{H_t} = f(enc_t {W_1}^{(b)} + \overleftarrow{H_{t-1}} {W_2}^{(b)} + {bias}^{(b)}), \quad (6)$$

where ${W_1}^{(b)}$, ${W_2}^{(b)}$, and ${bias}^{(b)}$ represent the parameters of the backward layer. Upon combining the hidden states from both layers, the resulting hidden state of the Bidirectional Long Short-Term Memory (BILSTM) is obtained. The output can be expressed using the following equation:

$$O_t = [\overrightarrow{H_t}, \overleftarrow{H_t}]W + bias. \quad (7)$$

Finally, the output becomes the input for the attention layer, leading to the production of the decoder output.

C. Critic

The employed critic takes the form of a two-layer feed-forward neural network, utilizing a ReLU activation function. The encoder output serves as the input for this critic network. The loss function hinges on the mean-square error between the network's output predictions and the actual rewards generated by the actor network.

During the training phase, we observed that the critic network can be effectively replaced with an exponential moving average, an approach used to estimate the local mean of a variable. By adopting this method, variable updates become intertwined with historical values over a specific timeframe, thereby enhancing the model's resilience. The mathematical formulation for this strategy is as follows:

$$V_t = \alpha V_{t-1} + (1 - \alpha)S_t, \quad (8)$$

where $\alpha \in (0, 1)$ and S_t represents the value at the t-th time step. This approach can effectively decrease processing time without compromising outcomes. This efficiency stems from the relatively straightforward nature of the critic network, which implies its impact is constrained. Furthermore, the employment of exponential moving averages can be regarded as a streamlined version of the critic network.

D. Reward

The reward serves as a metric to gauge the quality of the graph produced by the network. Consequently, the objective of either the actor network or the entire system is to maximize this reward. Notably, the Bayesian Information Criterion score (BIC) is extensively utilized in source-based causal discovery approaches due to its consistency and local consistency stemming from its decomposability [22]. Motivated by these attributes, we opt for BIC as our reward function, which the actor aims to maximize. For a given graph $\mathcal{G}$, its mathematical representation is as follows:

$$BIC(\mathcal{G}) = -2 \log p(\boldsymbol{X}; \widehat{\theta}, \mathcal{G}) + d_\theta \log m, \quad (9)$$

where θ is a set of parameters, d_θ is the dimensionality of θ, and $\widehat{\theta}$ is is the maximum likelihood estimation of θ.

In our approach, we adopt the acyclicity constraint formulated by Zheng et al. [23]. For a given binary adjacency matrix M representing a DAG $\mathcal{G}$, M remains acyclic when and only when $A(M) = 0$:

$$A(M) = trace(e^M) - d, \quad (10)$$

where e^M represents the matrix exponential of M. Thus, our reward function can be expressed in the following manner:

$$reward(\mathcal{G}) = -[BIC(\mathcal{G}) + \lambda A(M)], \quad (11)$$

where $\lambda \geq 0$ serves as a parameter subject to adjustment during training. In cases where ensuring acyclicity isn't a requisite for fMRI data, it's advised to set λ to a constant value of 0.

E. Estimating EC With FC Guidance

Studies indicate that FC can elucidate the presence of links between distinct brain regions; EC can reveal the effect of these links on behavioral and cognitive functions [25]. The exploration of functional brain connections lays the groundwork for investigating EC. We introduced an assisted learning approach employing FC as guidance for EC estimation to refine the precision of the brain's EC network.

We employed the Pearson correlation to establish the foundational structure of the causal diagram (FC network). This FC network subsequently guided the estimation of brain EC. The following sections elaborate on the sequential processes of the Pearson correlation and EC estimation.

Suppose the brain FC network derived from PC is denoted as W, and we have an element $w_{i,j} \in W$. This element, $w_{i,j}$, characterizes the statistical correlation between variables (brain regions) x_i and x_j. The calculation of $w_{i,j}$ follows this formulation:

$$w_{x_i,x_j} = \frac{\mathrm{cov}(x_i, x_j)}{\sigma_{x_i}\sigma_{x_j}}, \tag{12}$$

where cov(.) indicates the covariance between two variables, while σ_{x_i} and σ_{x_j} denote the standard deviations of variables x_i and x_j. The symmetry of $w_{i,j}$ and $w_{j,i}$ is upheld due to the FC network's lack of directionality, rendering it impervious to variations in the arrangement or magnitude of variables x_i and x_j.

From the insights of the obtained FC network, the FC network W acts as a query-key pair, and the EC network from deep reinforcement learning acts as the value vector. As a result, the predictive EC guided by the FC network can be formulated as follows:

$$G' = G \cdot \mathrm{Softmax}(W), \tag{13}$$

where $\cdot$ denotes dot product operation and $G \in \mathcal{G}$ signifies the EC network for an individual subject, mirroring the dimensionality of the FC network W in $\mathbb{R}^{n\times n}$. The resulting brain EC network of the subject is denoted as G'.

F. FGECRL Algorithm Description

In this section, we outline our novel algorithm in Algorithm 1. Following the parameter initialization, the actor-critic approach is utilized alongside generated graph scores, ensuring alignment of the projected optimal score within the [0, S_0] range. Furthermore, we enhance search space optimization by updating reward parameters at a frequency of t_0.

Algorithm 1 FGECRL Algorithm

Input : fMRI time series data X;Score parameters: S_L, S_U, S_0; penalty parameter λ, Δ; maximum number of iterations T; update frequency t_0
Output: Brain effective connectivity network
while $t \leq T$ **do**
  $graphs, Encoder \leftarrow Actor(X)$
  $Critic \leftarrow Critic(X)$
  $S \leftarrow BIC(graphs)$
  adjusting score $S \leftarrow S_0 \frac{S-S_L}{S_U-S_L}$
  $R \leftarrow Reward(S, graphs)$
  $loss \leftarrow Loss(R, Cri)$
  updating network parameters
  if $t \mod t_0 = 0$ **then**
    $S_U \leftarrow \min(S_U, S_min)$
    $\lambda \leftarrow \min(\lambda + \Delta, S_U)$
  end
end
Learn the FC by Pearson correlation as eq.12;
Estimate EC with the guidance of FC as eq.13;
return *Brain effective connectivity network*

IV. Results

A. Tinnitus Patients Data

Sound therapy treated 27 patients effectively (effective group, EG); 38 patients were not responsive to the treatment (ineffective group, IG), according to the improvement in the THI scores at week 24. No significant difference was found in the clinical factors among the EG, IG, and HCs (TableI). In addition, the changes in THI scores and the percentage improvement in THI scores were significantly different between the EG and IG (TableI).

Demographic data were compared using two sample t-tests, Chi-square test, or paired-sample t-tests.

B. Evaluation Metric and Statistical Analysis

The Accuracy was defined as the proportion of correct predictions of the positive and negative instances. It can be calculated by:

$$Accuracy = \frac{TP + TN}{TP + FP + TN + FN}, \tag{14}$$

where TP represents True Positives, the number of instances correctly predicted as positive; TN represents True Negatives, the number of instances correctly predicted as negative; FP represents False Positives, the number of instances falsely predicted as positive; and FN represents False Negatives, the number of instances falsely predicted as negative. It reflects the ability to differentiate subjects in different groups. A higher accuracy indicates better ability to identify the feature of functional connectivity. Taking into account the issue of imbalanced samples across different classes, we use the Balanced Accuracy Score (b-Accuracy) to evaluate the performance of a classification model. It can be calculated by:

$$b\text{-}Accuracy = \frac{1}{2} \times \left(\frac{TP}{TP + FN} + \frac{TN}{FP + TN}\right), \tag{15}$$

It calculates the average accuracy across all classes, where the accuracy of each class is determined by dividing the number of correctly classified samples in that class by the total number of samples in that class. A higher b-Accuracy indicates better performance of the model in handling imbalanced data.

We analyzed all of the possible connections of the nodes of the brain atlas. Results reflected the global measure of the connectivity. For the analysis of the ability of different

TABLE I
PATIENT DEMOGRAPHICS

	Tinnitus patients, Effective Group		Tinnitus patients, Ineffective Group		Healthy controls		*P-value*
	Baseline, n=27	Treated, n=27	Baseline, n=38	Treated, n=38	Baseline, n=28	6-months, n=28	
Age (years)	50.59 ± 11.79		47.42 ± 12.24		46.71 ± 7.90		0.375^a
Gender (male/female)	11/16		29/9		16/12		0.014^b
Handedness	27 right-handed		38 right-handed		28 right-handed		$> 0.99^a$
THI score	64.81 ± 23.23	31.63 ± 20.58	44.74 ± 20.92	50.16 ± 21.96	NA		$< 0.01^c$
ΔTHI score	33.19 ± 19.70		-5.42 ± 16.49		NA		NA
% improvement of THI score	52.11 ± 20.45		-19.66 ± 53.24		NA		NA
Duration, months	$\geq 6\& \leq 48$		$\geq 6\& \leq 48$		NA		NA
Tinnitus Pitch	$250 - 8,000$ Hz		$1,000 - 8,000$ Hz		NA		NA
Laterality	8 left, 4 right and 15 bilateral		12 left, 8 right and 18 bilateral		NA		0.756^b

[a] Two-sample t-tests.
[b] Chi-square test.
[c] Paired-sample t-tests.

methods that identify the feature of brain networks, we calculated the accuracy of each applied method, i.e. FC, EC, and FGECRL. Results were calculated between groups using Chi-square test. Paired Chi-square test was used for comparison of the same group of subject, e.g. EG before and after treatment. Chi-square test was used for comparison of different groups, e.g. EG versus HC.

Then we calculated the strength of effective connectivity in different brain regions. Comparisons among groups were performed by two sample t-tests or paired-sample t-tests. We constructed the FGEC network of the whole brain for different groups of subjects and demostrated the matrix of the network. For the comparison, we applied two-way mixed-model analysis of variance (ANOVA) and post hoc analyses.

SPSS 26 software (IBM Corp., Armonk, NY, USA) and R 4.2.1 (R Development Core Team) were used for statistical analysis. P values < 0.05 were considered statistically significant.

C. The Results of Classification

To verify the networks estimated by the FGECRL were discriminative in classification tasks, a set of classification experiments was conducted on the fMRI data of the patients with tinnitus (before and after treatment) and HCs. The study obtained EC networks using reinforcement learning (FGECRL without FC guidance, EC), FC networks using Pearson's correlation (PC), and new EC networks (FGECRL). Thus, the brain network of each participant can be identified using different methods. The study used the random forest method to classify EG, IG, and HC and the k-fold method for cross-validating the classification, with k set to 10.

The comparison results are shown in Figure 4 and Figure 5. The results of the FGECRL were better than those of the FC and EC methods under different circumstances. First, EC, FC, and FGECRL were used to differentiate tinnitus before and after treatment. For patients treated effectively (EG), the discrimination accuracies for the three methods were 36.36%, 44.32%, and 57.95%, the balance accuracies were 36.14%, 43.38%, and 59.29%, respectively (Figure 4A and Figure 5A). For patients who were not treated effectively (IG), the discrimination accuracies were 40.63% 39.84%, and 57.03%, the balance accuracies were 40.35% 41.31%, and

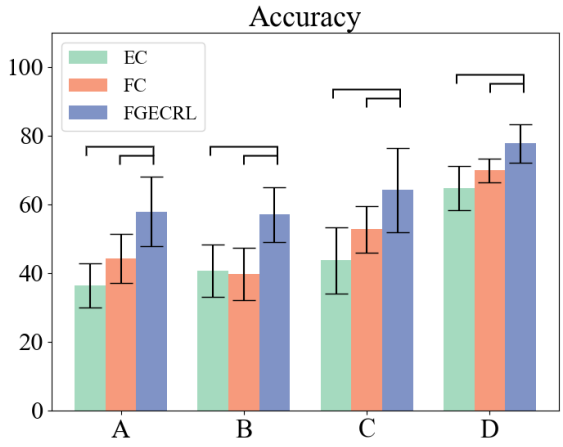

Fig. 4. The classification results accuracy of FC, EC, and FGECRL methods between groups. A, to differentiate EG before and after treatment, the accuracy of discrimination for the three methods was 36.36%, 44.32%, and 57.95%, respectively. B, to differentiate IG before and after treatment, the accuracy was 40.63% 39.84%, and 57.03%, respectively. C, to differentiate all of the patients in EG versus HC, the accuracy was 43.75%, 52.84%, and 64.20%, respectively. D, to differentiate all of the patients in IG versus HC, the accuracy was 64.81%, 69.91%, and 77.78%, respectively.

61.85%, respectively (Figure 4B and Figure 5B). Second, the ability of different methods to classify patients and HCs was compared. EC (43.75%) and FC (52.84%) have only moderate accuracy in discriminating between the EG and HCs. However, the FGECRL method can effectively discriminate between different groups of subjects with an accuracy of 64.02%, the balance accuracies were 49.56%, 56.46%, and 67.92%, which has the same trend (Figure 4C and Figure 5C). For IG and HC, the discrimination accuracies for EC, FC, and FGECRL were 64.81%, 69.91%, and 77.78%, the balance accuracies were 67.94%, 72.66%, and 79.49%, respectively (Figure 4D and Figure 5D). These results highlight the advantages of the FGECRL in identifying the brain network's directed information flow.

To clearly show the significant differences, we used the Friedman test and T test to attest to the significant difference between these methods. If the p-value obtained from the test is less than 0.05, we consider that a significant difference exists in the corresponding experimental results. In detail,

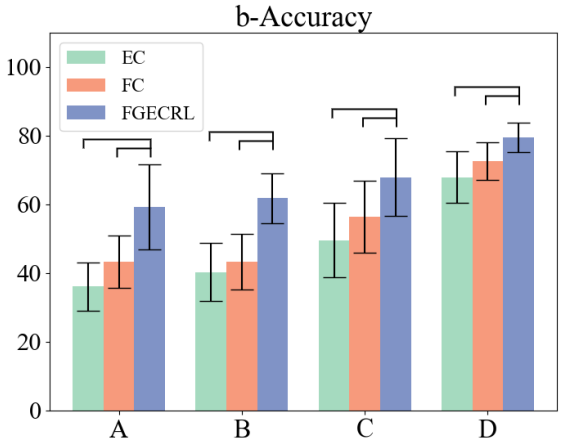

Fig. 5. The classification results b-Accuracy of FC, EC, and FGECRL methods between groups. A, to differentiate EG before and after treatment, the balance accuracy of discrimination for the three methods was 36.14%, 43.38%, and 59.29%, respectively. B, to differentiate IG before and after treatment, the accuracy was 40.35% 41.31%, and 61.85%, respectively. C, to differentiate all of the patients in EG versus HC, the accuracy was 49.56%, 56.46%, and 67.92%, respectively. D, to differentiate all of the patients in IG versus HC, the accuracy was 67.94%, 72.66%, and 79.49%, respectively. FC, functional connectivity; EC, effetive connectivity; FGECRL, functional-guided effective connectivity method based on reinforcement learning; EG, effective group; IG, ineffective group; HC, healthy controls.

we first performed the Friedman test on four groups, and the Friedman test indicates a significant difference between the three methods (6.29×10^{-3}, 3.23×10^{-2}, 6.97×10^{-3}, 5.48×10^{-3}). Furthermore, we performed the T test on the results of FGECRL and other methods, which are described in Figure 4 and Figure 5, we can find the FGECRL has a significant difference (better performance) compared to most other methods.

D. Effective Network Construction for Subject Groups

Our method was applied to construct the FGEC (functional-guided effective connectivity) network for each group of participants, including the EG before and after treatment, IG before and after treatment, and HCs. The ROIs of the human brainnetome atlas used in this study were grouped based on the connectional architecture, including anatomical and FC information (Supplementary TableI) [21].

Several grouped connectivity patterns were consistent with the connectional architecture of the brainnetome atlas. For example, the EG at baseline showed information output in the motor network (ROI 53–68, precentral gyrus and paracentral lobule), somatosensory network (ROI 155–162, postcentral gyrus), and visual network (ROI 189–198, medioventral occipital cortex). For these brain regions, no significant difference was found between the IG and HCs after effective treatment (Figure 6A to C). In contrast, less activated information flow was observed at baseline in the primary auditory cortex (ROI: 69 72) in the EG and IG than in the HC group. After treatment, the strength of the EC in the EG was similar to that of the HCs; the strength of the EC in the IG decreased (Figure 6D).

Inspired by previous studies [13], the differences in the lateral occipital cortex (ROI: 199–208) and thalamus (ROI: 231–246) were also investigated. However, no statistically significant differences were found between the groups (Figure 6E and F).

We constructed the FGEC network for EG before treatment, EG after treatmetn, IG before treatment, IG after treatment, and healthy controls. Figure 7 illustrates the pattern of FGEC networks of the five groups. The column represents information from one brain region to another; the row represents information from other brain regions. Hot colors indicate more information output; cold colors indicate less information communication. The matrix value represents the connectivity strength between the brain regions. The directional information flow was demonstrated because the matrix was not symmetrical.

As shown in Figure 7, the FGEC network pattern in patients with tinnitus was different from that in HC. In general, the alterations of the pattern in the connectional architecture in the EG at baseline was different from the other groups, featured by highlighted color in the columns that represent information output (Figure 7A). Results facilitate us to identify the subjects with better prognosis of treatment After effective treatment, the FGEC network features for the EG (Figure 7B) were similar to those of the HC (Figure 7E). However, the IG group's FGEC network pattern was not significantly altered before or after treatment (Figure 7 C and D).

V. Discussion

This study proposed a new method for identifying EC based on reinforcement learning. The FGECRL method could effectively delineates the features of the brain networks of different groups, better than the EC or FC alone. Thus, the patterns of information flow orchestration in patients with tinnitus before and after treatment were described more precise than ever before, providing new evidence for understanding the neural mechanisms of distinct treatment outcomes.

This study included five groups of participants (EG before and after treatment, IG before and after treatment, and HC). Changes in the fMRI signals before and after treatment were extremely subtle, possibly below the noise level, making it challenging to detect subtle differences when using the FC or EC methods alone. In addition, significant biological and neural differences of the participants added substantial variations in FC and EC signals between individuals. Also, in certain situations, precision is required to distinguish between different groups or detect minor changes. However, a single method, such as EC or FC alone, may not effectively handle these differences and fail to differentiate between the groups accurately. Combining different analytical methods or adopting more advanced techniques to enhance precision and sensitivity may be one of the solutions to better distinguish between groups in order to understand the effect of pre- and post-treatment fMRI signal changes in patients with tinnitus.

The key innovation of the proposed method lies in the setting of FC as a foundational step in exploring EC. Combining FC and EC can fully exploit the advantages of both analytical methods. As a functional integration method, FC measures the degree of whole-brain synchrony of the time series of blood oxygen level–dependent signals between distinct brain

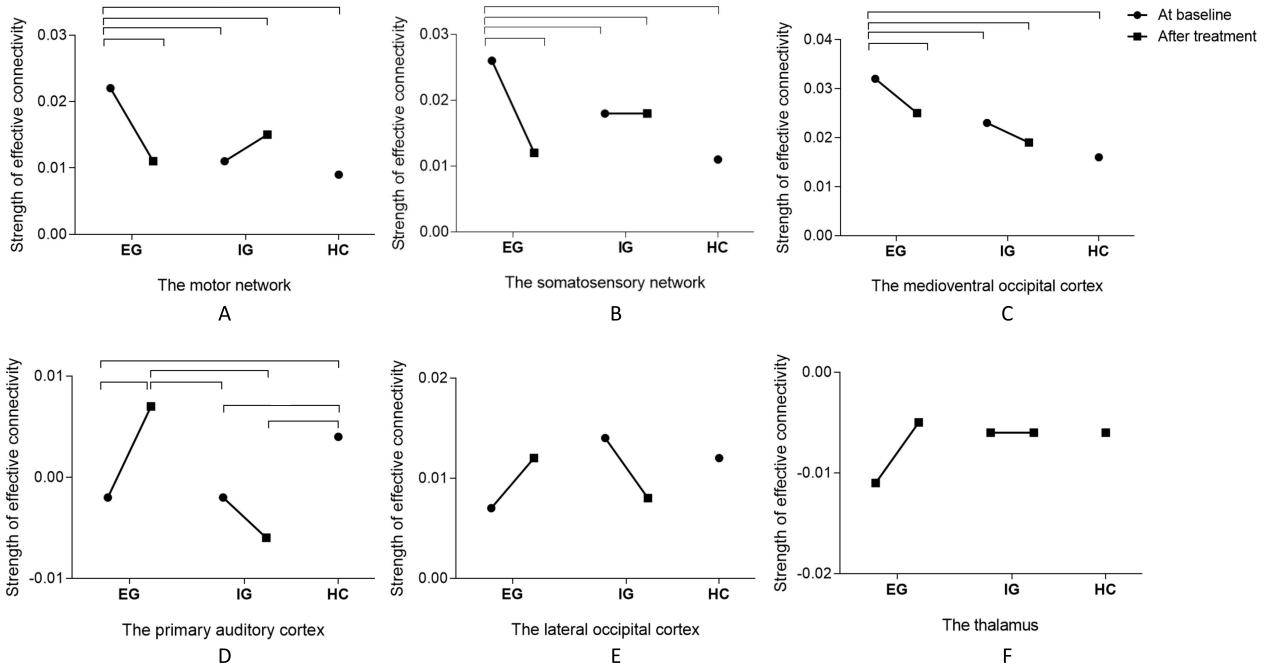

Fig. 6. Comparison of the strength of effective connectivity in different connectional architecture of brainnetome atlas among effective group (EG) before and after treatment, ineffective group (IG) before and after treatment, and healthy controls.

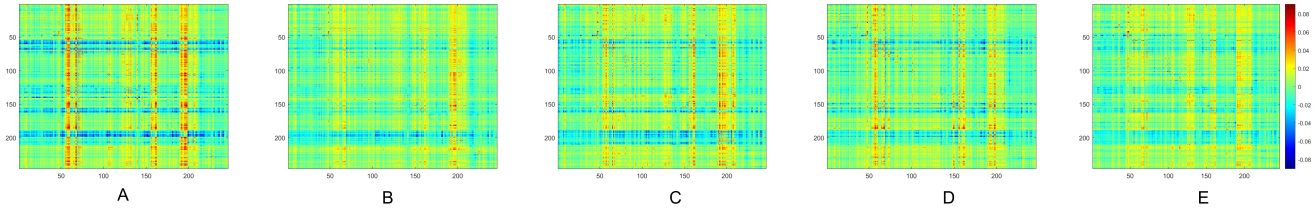

Fig. 7. The learned FGEC network for each group. A, effective group before treatment. B, effective group after treatment. C, ineffective group before treatment. D, ineffective group after treatment. E, healthy control group. FGEC, functional-guided effective connectivity.

regions, establishing the structural foundation for information transfer between distinct brain regions [24]. Research shows that FC and EC are associated [25], with stronger FC possibly implying stronger EC. However, there is lack of point-to-point correspondence; the presence of FC does not necessarily imply the existence of EC, and vice versa. Furthermore, EC is more discriminative than FC because it discerns the direction of information flow between different brain regions. Therefore, the study focused primarily on EC and utilized FC information to assist EC learning, enabling the algorithm to delineate the direction of information flow in the brain more finely and ultimately distinguish the differences in connectivity between different groups. The guidance of functional information increased the precision of the study results.

The proposed method has the potential of generalization. Functional MRI is an effective tool that can provide key data information not only for the research on mechanism of mental disorders [26], but also for the treatment effect prediction or evaluation [27], [28]. However, classical analytic methods cannot provide information about the direction of connectivity [24], which may lead to missing or ignoring critical information. Effective connectivity provided additional information that can characterize the direction of information flow within functional connectivity architecture. Our proposed FGECRL method is a candidate tool to characterize the architecture of neural network, thus providing key information for the analysis of brain networks for different kinds of subjects.

Results were further validated when compared with previous findings. Consistent with previous results [13], altered information flow was detected in the motor network, somatosensory network, and medioventral occipital cortex of patients with tinnitus at baseline. As a phantom sensation, tinnitus is characterized by abnormal motor cortex excitability [29]. Neural changes in auditory sensation can induce changes in the motor network via cross-modal plasticity [30]. Even comorbid conditions of tinnitus, such as anxiety or affective disorders, may correlate with motor cortex excitability, and it has been proven that effective therapeutic interventions are correlated with decreased activity of the motor network [31]. Similarly, the somatosensory network may also be activated by possible tinnitus etiologies [32]. According to our results, the enhanced activity of the motor network, somatosensory network, and medioventral occipital cortex decreased to the normal range, similar to that in HCs. These findings may represent crucial changes for the effective treatment of tinnitus

and provide clues for extending the findings of previous studies [33].

EC of the primary auditory cortex was complicated in both groups. Successfully treated patients with tinnitus show increased regional brain volume and neural activity [34]. As a core brain region in the gain model [35], [36], reduced information flow in the auditory cortex may represent a lack of central neural gain in patients with tinnitus. After treatment, rehabilitation of EC to the normal range was observed in the EG but not in the IG. These results support the theory of increased central neural gain in the auditory system [37]. Without a balance of Bayesian inferences among the brain regions related to the perception of tinnitus, the sound of silence would be far from reaching [38], [39]. Consequently, the EC of the primary auditory cortex may be a suitable model for effective sound therapy.

The functional connectivity of thalamus and occipital cortex were reported as the features of tinnitus [13]. However, there was no statistical significance regarding the EC of the thalamus or lateral occipital cortex in this study, possibly because the more precise FGECRL method was used for identifying the brain EC. For the thalamus, the enhanced connectivity in the EG after effective treatment may represent recovered gating function, according to the gating theory of tinnitus [40]. However, several studies have failed to identify structural or functional changes in the thalamus before and after treatment [41]. Regional activity and oscillations may be more sensitive than FC with other brain regions [42]. For possible neuromodulatory targets for treatment, further studies should focus on regional activity rather than the connectivity of the thalamus when analyzing the neural mechanism of effective treatment.

Another explanation is possible for the insignificant changes in EC of the thalamus. Our method only demonstrated either the output or input of information for a brain region. It is the limitation of the FGECRL method. This method was not able to report bidirectional information flow. However, a study has indicated both increased and decreased FC of the thalamus in different brain regions following effective treatment [43]. It may because of the average effect that the results were not statistically significant among the groups. The limitation should be noted when interpreting the results.

VI. Conclusion

This study proposed a new FGECRL method to delineate EC precisely among tinnitus patients with distinct treatment outcomes. The pattern of the FGEC network can be regarded as direct evidence of the effectiveness of sound therapy in patients with tinnitus. Effective treatment was characterized by a similar pattern of FGEC networks between patients with tinnitus after treatment and HCs. Deactivated information output in the motor network, somatosensory network, and medioventral occipital cortex may be biological indicators of effective treatment. The maintenance of decreased EC in the primary auditory cortex may represent a failure of sound therapy, further supporting the causal inference theory for the perception of tinnitus.

References

[1] C. A. Bauer, "Tinnitus," *New England J. Med.*, vol. 378, no. 13, pp. 1224–1231, 2018.

[2] Y.-F. Cheng, S. Xirasagar, N.-W. Kuo, and H.-C. Lin, "Tinnitus and risk of attempted suicide: A one year follow-up study," *J. Affect. Disorders*, vol. 322, pp. 141–145, Feb. 2023.

[3] D. E. Tunkel et al., "Clinical practice guideline: Tinnitus," *Otolaryngology–Head Neck Surgery*, vol. 151, no. 2, pp. S1–S40, 2014.

[4] M. Pienkowski, "Rationale and efficacy of sound therapies for tinnitus and hyperacusis," *Neuroscience*, vol. 407, pp. 120–134, May 2019.

[5] G. D. Searchfield, M. Durai, and T. Linford, "A state-of-the-art review: Personalization of tinnitus sound therapy," *Frontiers Psychol.*, vol. 8, p. 1599, Sep. 2017.

[6] T. E. Kok et al., "Resting-state networks in tinnitus: A scoping review," *Clin. Neuroradiology*, vol. 32, no. 4, pp. 903–922, Dec. 2022.

[7] M. E. Adams, T. C. Huang, S. Nagarajan, and S. W. Cheung, "Tinnitus neuroimaging," *Otolaryngologic Clinics North Amer.*, vol. 53, no. 4, pp. 583–603, 2020.

[8] Z. Liu et al., "Generalizable sample-efficient Siamese autoencoder for tinnitus diagnosis in listeners with subjective tinnitus," *IEEE Trans. Neural Syst. Rehabil. Eng.*, vol. 29, pp. 1452–1461, 2021.

[9] X. Yu et al., "Effect of acupuncture treatment on cortical activation in patients with tinnitus: A functional near-infrared spectroscopy study," *IEEE Trans. Neural Syst. Rehabil. Eng.*, vol. 31, pp. 729–737, 2023.

[10] F. T. Husain and R. A. Khan, "Review and perspective on brain bases of tinnitus," *J. Assoc. Res. Otolaryngology*, vol. 24, no. 6, pp. 549–562, Nov. 2023.

[11] Q. Chen et al., "Distinct brain structural-functional network topological coupling explains different outcomes in tinnitus patients treated with sound therapy," *Human Brain Mapping*, vol. 43, no. 10, pp. 3245–3256, Jul. 2022.

[12] D. M. Khan, N. Yahya, N. Kamel, and I. Faye, "A novel method for efficient estimation of brain effective connectivity in EEG," *Comput. Methods Programs Biomed.*, vol. 228, Jan. 2023, Art. no. 107242.

[13] H. Lv et al., "Brain effective connectivity analysis facilitates the treatment outcome expectation of sound therapy in patients with tinnitus," *IEEE Trans. Neural Syst. Rehabil. Eng.*, vol. 31, pp. 1158–1166, 2023.

[14] J. Ji, A. Zou, J. Liu, C. Yang, X. Zhang, and Y. Song, "A survey on brain effective connectivity network learning," *IEEE Trans. Neural Netw. Learn. Syst.*, vol. 34, no. 4, pp. 1879–1899, Apr. 2023.

[15] J. Ji, Z. Zhang, L. Han, and J. Liu, "MetaCAE: Causal autoencoder with meta-knowledge transfer for brain effective connectivity estimation," *Comput. Biol. Med.*, vol. 170, Mar. 2024, Art. no. 107940.

[16] J. Liu, J. Ji, G. Xun, L. Yao, M. Huai, and A. Zhang, "EC-GAN: Inferring brain effective connectivity via generative adversarial networks," *Proc. AAAI Conf. Artif. Intell.*, vol. 34, no. 4, pp. 4852–4859, Apr. 2020.

[17] J. Ji, L. Han, F. Wang, and J. Liu, "Dynamic effective connectivity learning based on nonparametric state estimation and GAN," *IEEE Trans. Instrum. Meas.*, vol. 73, pp. 1–12, 2024.

[18] H. Li, S. Yu, and J. Principe, "Causal recurrent variational autoencoder for medical time series generation," 2023, *arXiv:2301.06574*.

[19] F. Zeman et al., "Tinnitus handicap inventory for evaluating treatment effects: Which changes are clinically relevant?" *Otolaryngology–Head Neck Surgery*, vol. 145, no. 2, pp. 282–287, Aug. 2011.

[20] J. Wang, X. Wang, M. Xia, X. Liao, A. Evans, and Y. He, "GRETNA: A graph theoretical network analysis toolbox for imaging connectomics," *Frontiers Hum. Neurosci.*, vol. 9, p. 386, Jun. 2015.

[21] L. Fan et al., "The human brainnetome atlas: A new brain atlas based on connectional architecture," *Cerebral Cortex*, vol. 26, no. 8, pp. 3508–3526, 2016.

[22] S. Zhu, I. Ng, and Z. Chen, "Causal discovery with reinforcement learning," in *Proc. Int. Conf. Learn. Represent.*, 2019, pp. 1–17.

[23] X. Zheng, B. Aragam, P. K. Ravikumar, and E. P. Xing, "DAGs with NO TEARS: Continuous optimization for structure learning," in *Proc. Adv. Neural Inf. Process. Syst.*, vol. 31, 2018, pp. 1–12.

[24] H. Lv et al., "Resting-state functional MRI: Everything that nonexperts have always wanted to know," *Amer. J. Neuroradiology*, pp. 1390–1399, Jan. 2018.

[25] A. T. Reid et al., "Advancing functional connectivity research from association to causation," *Nature Neurosci.*, vol. 22, no. 11, pp. 1751–1760, Nov. 2019.

[26] Y. Massalha, E. Maggioni, A. Callari, P. Brambilla, and G. Delvecchio, "A review of resting-state fMRI correlations with executive functions and social cognition in bipolar disorder," *J. Affect. Disorders*, vol. 334, pp. 337–351, Aug. 2023.

[27] S. Baxendale, "What are we really predicting with fMRI in epilepsy surgery?" *Epilepsy Behav.*, vol. 145, Aug. 2023, Art. no. 109298.

[28] L. S. Dominicus et al., "FMRI connectivity as a biomarker of antipsychotic treatment response: A systematic review," *NeuroImage: Clin.*, vol. 40, 2023, Art. no. 103515.

[29] E. M. Khedr, J. C. Rothwell, M. A. Ahmed, E. M. Awad, and O. Galal, "Cortical excitability and transcallosal inhibition in chronic tinnitus: Transcranial magnetic study," *Neurophysiologie Clinique/Clinical Neurophysiology*, vol. 38, no. 4, pp. 243–248, Aug. 2008.

[30] D. Bavelier and H. J. Neville, "Cross-modal plasticity: Where and how?" *Nature Rev. Neurosci.*, vol. 3, no. 6, pp. 443–452, Jun. 2002.

[31] M. Schecklmann et al., "State- and trait-related alterations of motor cortex excitability in tinnitus patients," *PLoS ONE*, vol. 9, no. 1, Jan. 2014, Art. no. e85015.

[32] H. F. Haider et al., "Pathophysiology, diagnosis and treatment of somatosensory tinnitus: A scoping review," *Frontiers Neurosci.*, vol. 11, p. 207, Apr. 2017.

[33] H. Lv et al., "Sound therapy can modulate the functional connectivity of the auditory network," *Prog. Neuro-Psychopharmacology Biol. Psychiatry*, vol. 110, Aug. 2021, Art. no. 110323.

[34] C. M. Krick, M. Grapp, J. Daneshvar-Talebi, W. Reith, P. K. Plinkert, and H. V. Bolay, "Cortical reorganization in recent-onset tinnitus patients by the Heidelberg model of music therapy," *Frontiers Neurosci.*, vol. 9, p. 49, Feb. 2015.

[35] A. Henton and T. Tzounopoulos, "What's the buzz? The neuroscience and the treatment of tinnitus," *Physiological Rev.*, vol. 101, no. 4, pp. 1609–1632, Oct. 2021.

[36] W. Sedley, "Tinnitus: Does gain explain?" *Neuroscience*, vol. 407, pp. 213–228, May 2019.

[37] B. Hofmeier et al., "Reduced sound-evoked and resting-state BOLD fMRI connectivity in tinnitus," *NeuroImage: Clin.*, vol. 20, pp. 637–649, 2018.

[38] D. De Ridder, K. Joos, and S. Vanneste, "The enigma of the tinnitus-free dream state in a Bayesian world," *Neural Plasticity*, vol. 2014, pp. 1–5, Jul. 2014.

[39] D. De Ridder, S. Vanneste, and W. Freeman, "The Bayesian brain: Phantom percepts resolve sensory uncertainty," *Neurosci. Biobehavioral Rev.*, vol. 44, pp. 4–15, Jul. 2014.

[40] P. Brinkmann, S. A. Kotz, J. V. Smit, M. L. F. Janssen, and M. Schwartze, "Auditory thalamus dysfunction and pathophysiology in tinnitus: A predictive network hypothesis," *Brain Struct. Function*, vol. 226, no. 6, pp. 1659–1676, Jul. 2021.

[41] Q. Chen et al., "Brain structural and functional reorganization in tinnitus patients without hearing loss after sound therapy: A preliminary longitudinal study," *Frontiers Neurosci.*, vol. 15, Mar. 2021, Art. no. 573858.

[42] F. Almasabi et al., "The role of the medial geniculate body of the thalamus in the pathophysiology of tinnitus and implications for treatment," *Brain Res.*, vol. 1779, Mar. 2022, Art. no. 147797.

[43] H. Lv et al., "Altered functional connectivity of the thalamus in tinnitus patients is correlated with symptom alleviation after sound therapy," *Brain Imag. Behav.*, vol. 14, no. 6, pp. 2668–2678, Dec. 2020.